

Received 10 July 2025

Accepted 22 September 2025

Edited by M. Weil, Vienna University of Technology, Austria

**Keywords:** crystal structure; Hirshfeld surface analysis; vibrational spectroscopy; methyl chloroformate.**CCDC references:** 2490420; 2490419**Supporting information:** this article has supporting information at journals.iucr.org/e

# Crystal structure of methyl chloroformate

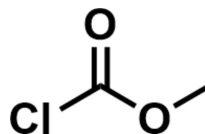
Sven Ringelband and Frank Tambornino\*

Philipps-Universität Marburg, Hans-Meerwein-Str. 4, 35032 Marburg, Germany. \*Correspondence e-mail: frank.tambornino@chemie.uni-marburg.de

The crystal structure of methyl chloroformate,  $C_2H_3ClO_2$ , was determined by single-crystal X-ray diffraction data at 200 and 100 K. A suitable single crystal was grown in a capillary directly on the goniometer *via* Ostwald ripening around its melting point at 210 K. The  $ClC(O)OCH_3$  molecule has a staggered conformation and is planar (without H atoms) with point group  $C_s$ . In the crystal, methyl chloroformate features weak  $Cl \cdots O$  interactions forming chains along [100], which again extend into a network *via* intermolecular  $C \cdots O$  dipole interactions, consistent with Hirshfeld surface analysis. Complementary quantum chemical calculations at the DFT-def2-TZVP/PBE0-D3 level of theory were performed to compare with the experimental Raman data in both the liquid and solid state.

## 1. Chemical context

Methyl chloroformate,  $ClC(O)OCH_3$ , is a liquid at room temperature with a melting point of 212 K (GESTIS, 2025). It is widely used in organic chemistry to introduce a methoxy-carbonyl functionality to a suitable nucleophile (Chiarucci *et al.*, 2012). Methyl chloroformate is well characterized, including its conformational properties by vibrational spectroscopy, microwave spectra (Groner *et al.*, 1990), and gas phase electron diffraction (O’Gorman *et al.*, 1950). Herein, we report on its hitherto unknown crystal structure on the basis of diffraction data recorded at 200 and 100 K. Additional quantum chemical calculations were performed and are consistent with the experimental findings and allow for the assignment of the vibrational modes.



## 2. Structural commentary

Methyl chloroformate crystallizes in the orthorhombic crystal system with the centrosymmetric space group  $Pnma$ . It has been shown that crystals of small molecular compounds can exhibit extensive polymorphism in the solid state, thus undergoing phase transitions at temperatures somewhere below their melting temperatures (Cruz-Cabeza *et al.*, 2015). However, lowering the temperature starting from 200 K did not lead to a phase transition. The unit cell contains four formula units ( $Z = 4$ ) and one independent molecule in the asymmetric unit (Fig. 1). In the crystal structure, individual molecules are arranged in an  $AB$  stacking pattern (Fig. 2).

In the solid state,  $ClC(O)OCH_3$  adopts  $C_s$  symmetry with the molecule lying on a mirror plane and thus displaying a

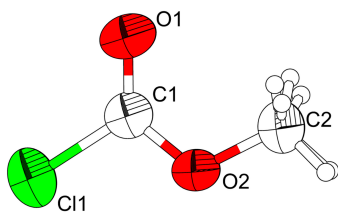


**Table 1**

Comparison of selected interatomic distances ( $\text{\AA}$ ,  $^\circ$ ) of methyl chloroformate (X-ray, this work), methyl chloroformate (electron diffraction; O'Gorman *et al.*, 1950), phosgene (Zaslow *et al.*, 1952) and dimethyl carbonate (Whitfield, 2023).

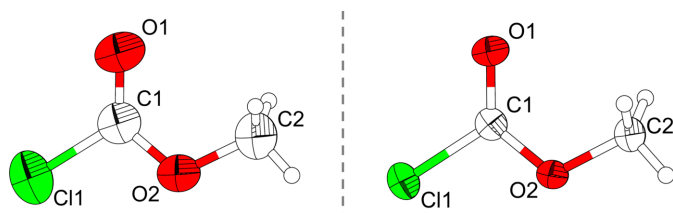
	X-ray 200 K	X-ray 100 K	Electron diffraction	Phosgene	Dimethyl carbonate 82 K
C=O	1.186 (2)	1.195 (2)	1.19 (3)	1.15 (2)	1.219 (2)
C–Cl	1.7504 (13)	1.7502 (13)	1.75 (2)	1.74 (2)*	–
(CO)–O	1.306 (2)	1.309 (2)	1.36 (4)	–	1.337 (2)*
O–CH <sub>3</sub>	1.456 (2)	1.462 (2)	1.47 (4)	–	1.456 (2)*
Cl–C=O	122.46 (10)	122.47 (10)	–	124(1.5)*	–
Cl–C–O	108.61 (9)	108.75 (9)	112 (3)	–	–
O=C–O	128.93 (11)	128.78 (11)	126 (4)	–	125.58 (11)*

\*Mean values.

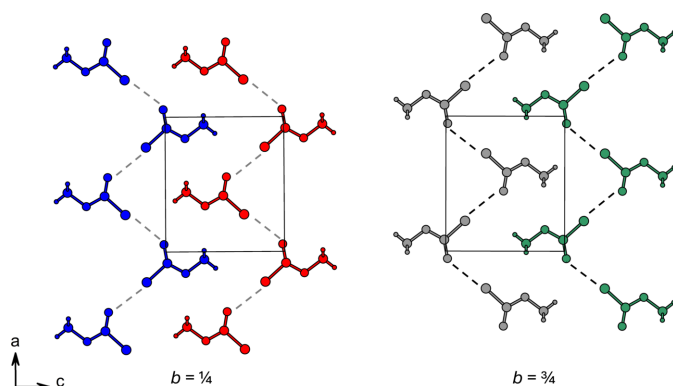
torsion angle Cl1–C1–O2–C2 of exactly  $180^\circ$ . Due to the symmetry restrictions of point group  $C_s$ , the methyl group is in a staggered orientation with respect to the carbonyl group. Also, the O–CH<sub>3</sub> moiety is orientated *syn* relative to the C=O bond, with bond lengths similar to those determined by electron diffraction and comparable to those of phosgene (Zaslow *et al.*, 1952) and dimethyl carbonate (Whitfield, 2023). A comparison of the structural parameters is given in Table 1.

### 3. Supramolecular features

The crystal packing of methyl chloroformate is dominated by short intermolecular Cl $\cdots$ O contacts with a distance of  $d_{\text{Cl}\cdots\text{O}} = 3.0442(9) \text{ \AA}$ , forming infinite chains along [100] (Fig. 2). Within these chains, the molecules are aligned in a zigzag fashion. However, individual chains are not interconnected


**Figure 1**

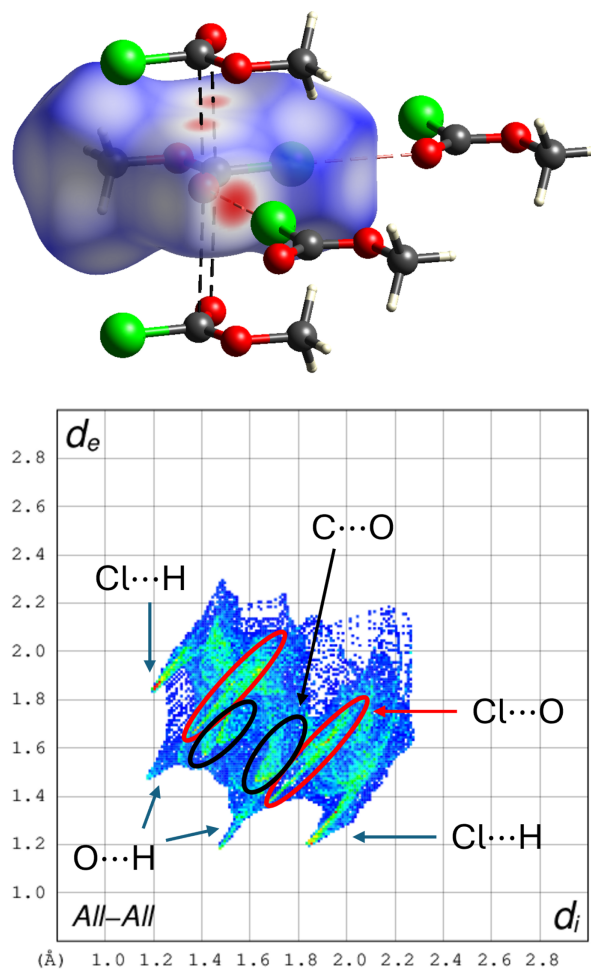
Molecular structure of a methyl chloroformate molecule in the solid state measured at 200 K (left) and 100 K (right). Atoms are drawn with displacement ellipsoids at the 70% probability level.


**Figure 2**

AB stacking in the crystal structure of methyl chloroformate viewed along [010]. Repeating layers: A (left) and B (right).

into layers, but instead form a framework through weak intermolecular dipole interactions between the carbonyl oxygen atom and the central carbon atom of two parallel molecules along [010].

A Hirshfeld surface analysis was performed using *Crystal-Explorer* (Spackman *et al.*, 2021) to quantify and visualize the intermolecular interactions in the crystal structure of the title compound. The Hirshfeld surface was mapped with the  $d_{\text{norm}}$  function (Fig. 3), highlighting attractive interactions shorter


**Figure 3**

Hirshfeld surface (top) and fingerprint plot (bottom) mapped for methyl chloroformate on basis of 100 K data. Red areas indicate short contacts shorter than the sum of the van der Waals radii. Color code: C gray, O red, Cl green, H white.

**Table 2**

 Vibrational band positions ( $\text{cm}^{-1}$ ) and band assignments of the Raman spectra of liquid and solid methyl chloroformate based on the DFT calculation. Symmetry modes are given in parentheses.

$\nu_{\text{calc.}}$	$\nu_{\text{obs.}}(\text{liquid})$	$\nu_{\text{obs.}}(\text{solid})$	Assignment	$\nu_{\text{calc.}}$	$\nu_{\text{obs.}}(\text{liquid})$	$\nu_{\text{obs.}}(\text{solid})$	Assignment
182 ( $B_{2g}$ )	–	195	out-of-plane $\delta(\text{C}-\text{O}-\text{C})$	1248 ( $A_g$ )	1206	1206	$\nu(\text{C}-\text{O})+\delta(\text{CH}_3)$
191 ( $B_{1g}$ )	–	–	–	1253 ( $B_{3g}$ )	–	–	–
272 ( $B_{3g}$ )	281	283	in-plane $\delta(\text{C}-\text{O}-\text{C})$	1470 ( $B_{3g}$ )	1457	1435	$\delta_s(\text{CH}_3)$
272 ( $A_g$ )	–	–	–	1474 ( $A_g$ )	–	–	–
409 ( $B_{3g}$ )	407	411	in-plane $\delta(\text{C}-\text{O}-\text{C}-\text{Cl})$	1485 ( $A_g$ )	–	1452	$\delta_s(\text{CH}_3)$
410 ( $A_g$ )	–	–	–	1486 ( $B_{3g}$ )	–	–	–
488 ( $A_g$ )	485	481	$\nu(\text{C}-\text{Cl})$	1491 ( $B_{1g}$ )	–	1459	$\delta_{\text{as}}(\text{CH}_3)$
490 ( $B_{3g}$ )	–	486	–	1494 ( $B_{2g}$ )	–	–	–
719 ( $B_{1g}$ )	–	–	out-of-plane $\nu_{\text{as}}(\text{O}-\text{C}-\text{O})$ wagging	1875 ( $A_g$ )	1788	1756	$\nu(\text{C}=\text{O})$
723 ( $B_{2g}$ )	–	–	–	1884 ( $B_{3g}$ )	–	1778	–
845 ( $A_g$ )	823	824	$\delta(\text{C}-\text{O}-\text{C}-\text{Cl})$ scissoring	3087 ( $A_g$ )	2967	2964	$\nu_s(\text{CH}_3)$
852 ( $B_{3g}$ )	–	–	–	3088 ( $B_{3g}$ )	–	–	–
996 ( $A_g$ )	950	950	$\nu(\text{O}-\text{CH}_3)$	3180 ( $B_{2g}$ )	3026	3029	$\nu_{\text{as}}(\text{CH}_3)$
1004 ( $B_{3g}$ )	–	975	–	3180 ( $B_{1g}$ )	–	–	–
1174 ( $B_{1g}$ )	1155	1148	$\delta(\text{CH}_3)$ rocking	3222 ( $A_g$ )	3053	3056	$\nu_{\text{as}}(\text{CH}_3)$
1175 ( $B_{2g}$ )	–	–	–	3222 ( $B_{3g}$ )	–	–	–
1198 ( $A_g$ )	–	1155	$\delta(\text{CH}_3)$ rocking	–	–	–	–
1212 ( $B_{3g}$ )	–	1168	–	–	–	–	–

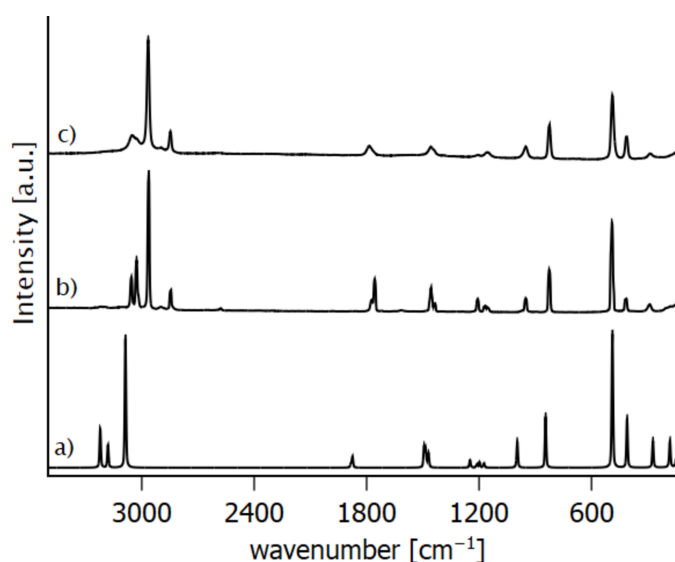
 Notes:  $\nu$  = stretching vibration,  $\delta$  = bending vibration,  $s$  = symmetric,  $as$  = asymmetric, – = not observed.

than the sum of the van der Waals radii in red and equal or longer contacts in white and blue, respectively. Akin to the observations above, relevant contributions arise from  $\text{Cl}\cdots\text{O}$  and  $\text{C}\cdots\text{O}$  short contacts accounting for only 12.6% and 7.6% to the overall Hirshfeld plot. Other major contributions include  $\text{Cl}-\text{H}$  (35.0%) and  $\text{O}-\text{H}$  (27.4%) intermolecular contacts. However, those are equal to or longer than the sum of their van der Waals radii.

#### 4. Vibrational spectroscopy

Experimental Raman spectra of liquid and solid methyl chloroformate were recorded at room temperature and at

153 K, confirming the molecular structure as determined by X-ray analysis. The experimental spectra are confirmed by quantum chemical calculations at the DFT-def2-TZVP/PBE0-D3 level of theory (Weigend & Ahlrichs, 2005; Karttunen *et al.*, 2015; Dovesi *et al.*, 2018; Zicovich *et al.*, 2004; Pascale *et al.*, 2004; Maschio *et al.*, 2013; Grimme *et al.*, 2010) on the basis of the crystal structure of methyl chloroformate. The recorded and calculated spectra are in good agreement, as shown in Fig. 4. The vibrational frequencies have been calculated within the harmonic approximation and therefore are overestimated, especially at higher wavenumbers. Nevertheless, the vibrational band at  $2845\text{ cm}^{-1}$  is not reproduced in the calculated spectrum. A comparison of calculated and observed vibrational bands is given in Table 2.


**Figure 4**

Calculated (*a*) and recorded Raman spectra of methyl chloroformate (*b*) at room temperature (liquid) and (*c*) at 153 K (crystalline). Calculated Raman spectra of solid  $\text{ClC}(\text{O})\text{OCH}_3$  at the DFT-TZVP/PBE0 level of theory.

#### 5. Synthesis and crystallization

Methyl chloroformate (Fisher Scientific GmbH, 99%) was used as received. Its purity was checked with vibrational IR and Raman spectroscopy. A borosilicate glass capillary (0.3 mm, Hilgenberg) was filled with a small amount of methyl chloroformate and flame-sealed at ambient pressure. The capillary was mounted onto the goniometer of the diffractometer and shock-cooled at 100 K using an open-flow cryostat to obtain a polycrystalline sample. The sample was incrementally heated at a rate of  $180\text{ K min}^{-1}$  until partial melting was observed at around 213 K. Subsequently, a suitable single crystal was grown through Ostwald ripening between 200 and 213 K in three cycles. Full datasets were collected at 200 and 100 K and reflections of the strongest scattering individual were integrated.

#### 6. Refinement

Crystal data, data collection and structure refinement details are summarized in Table 3. The positions of the hydrogen

**Table 3**

Experimental details.

	100 K	200 K
Crystal data		
Chemical formula	C <sub>2</sub> H <sub>3</sub> ClO <sub>2</sub>	C <sub>2</sub> H <sub>3</sub> ClO <sub>2</sub>
<i>M<sub>r</sub></i>	94.49	94.49
Crystal system, space group	Orthorhombic, <i>Pnma</i>	Orthorhombic, <i>Pnma</i>
<i>a</i> , <i>b</i> , <i>c</i> (Å)	8.4404 (5), 6.2019 (4), 7.4314 (4)	8.526 (2), 6.3454 (15), 7.4619 (16)
<i>V</i> (Å <sup>3</sup> )	389.01 (4)	403.67 (16)
<i>Z</i>	4	4
Radiation type	Cu <i>Kα</i>	Cu <i>Kα</i>
$\mu$ (mm <sup>-1</sup> )	7.23	6.97
Crystal size (mm)	0.30 × 0.05 (radius)	0.30 × 0.15 (radius)
Data collection		
Diffractometer	Stoe Stadivari	Stoe Stadivari
Absorption correction	Multi-scan ( <i>LANA</i> ; Koziskova <i>et al.</i> , 2016)	Multi-scan ( <i>LANA</i> ; Koziskova <i>et al.</i> , 2016)
<i>T<sub>min</sub></i> , <i>T<sub>max</sub></i>	0.161, 0.337	0.231, 0.512
No. of measured, independent and observed [ <i>I</i> > 2σ( <i>I</i> )] reflections	8421, 432, 415	10088, 453, 432
<i>R<sub>int</sub></i>	0.018	0.022
(sin θ/λ) <sub>max</sub> (Å <sup>-1</sup> )	0.627	0.625
Refinement		
<i>R</i> [ <i>F</i> <sup>2</sup> > 2σ( <i>F</i> <sup>2</sup> )], <i>wR</i> ( <i>F</i> <sup>2</sup> ), <i>S</i>	0.018, 0.049, 1.08	0.022, 0.064, 1.11
No. of reflections	432	453
No. of parameters	38	39
H-atom treatment	All H-atom parameters refined	All H-atom parameters refined
Δρ <sub>max</sub> , Δρ <sub>min</sub> (e Å <sup>-3</sup> )	0.18, -0.17	0.18, -0.16

Computer programs: *X-AREA* (Stoe, 2022), *SHELXT* (Sheldrick, 2015a), *SHELXL* (Sheldrick, 2015b) and *OLEX2* (Dolomanov *et al.*, 2009).

atoms were obtained through difference-Fourier synthesis in both datasets.

### Funding information

The authors thank the DFG for financial support (TA 1357/5-1).

### References

Chiarucci, M., di Lillo, M., Romaniello, A., Cozzi, P. G., Cera, G. & Bandini, M. (2012). *Chem. Sci.* **3**, 2859–2863.  
 Cruz-Cabeza, A. J., Reutzel-Edens, S. M. & Bernstein, J. (2015). *Chem. Soc. Rev.* **44**, 8619–8635.  
 Dolomanov, O. V., Bourhis, L. J., Gildea, R. J., Howard, J. A. K. & Puschmann, H. (2009). *J. Appl. Cryst.* **42**, 339–341.  
 Dovesi, R., Erba, A., Orlando, R., Zicovich-Wilson, C. M., Civalleri, B., Maschio, L., Rérat, M., Casassa, S., Baima, J., Salustro, S. & Kirtman, B. (2018). *WIREs Comput. Mol. Sci.* **8**, e1360.  
 GESTIS (2025). Entry on methyl chloroformate in the GESTIS Substance Database des IFA, accessed 22 July 2025, <https://gestis.dguv.de/data?name=027050>.  
 Grimme, S., Antony, J., Ehrlich, S. & Krieg, H. A. (2010). *J. Chem. Phys.* **132**, 154104.

Groner, P., Tolley, C. L. & Durig, J. R. (1990). *Chem. Phys.* **142**, 381–394.  
 Karttunen, A. J., Tynell, T. & Karppinen, M. (2015). *J. Phys. Chem. C* **119**, 13105–13114.  
 Koziskova, J., Hahn, F., Richter, J. & Kožíšek, J. (2016). *Acta Chim. Slovaca* **9**, 136–140.  
 Maschio, L., Kirtman, B., Rérat, M., Orlando, R. & Dovesi, R. (2013). *J. Chem. Phys.* **139**, 164102.  
 O’Gorman, J. M., Shand, W. & Schomaker, V. (1950). *J. Am. Chem. Soc.* **72**, 4222–4228.  
 Pascale, F., Zicovich-Wilson, C. M., López Gejo, F., Civalleri, B., Orlando, R. & Dovesi, R. (2004). *J. Comput. Chem.* **25**, 888–897.  
 Sheldrick, G. M. (2015a). *Acta Cryst.* **A71**, 3–8.  
 Sheldrick, G. M. (2015b). *Acta Cryst.* **C71**, 3–8.  
 Spackman, P. R., Turner, M. J., McKinnon, J. J., Wolff, S. K., Grimwood, D. J., Jayatilaka, D. & Spackman, M. A. (2021). *J. Appl. Cryst.* **54**, 1006–1011.  
 Stoe (2022). *X-AREA*. Stoe & Cie GmbH, Darmstadt, Germany.  
 Weigend, F. & Ahlrichs, R. (2005). *Phys. Chem. Chem. Phys.* **7**, 3297–3305.  
 Whitfield, P. S. (2023). *Powder Diffr.* **38**, 100–111.  
 Zaslav, B., Atoji, M. & Lipscomb, W. N. (1952). *Acta Cryst.* **5**, 833–837.  
 Zicovich-Wilson, C. M., Pascale, F., Roetti, C., Saunders, V. R., Orlando, R. & Dovesi, R. (2004). *J. Comput. Chem.* **25**, 1873–1881.

## supporting information

*Acta Cryst.* (2025). E81, 987-990 [https://doi.org/10.1107/S2056989025008369]

## Crystal structure of methyl chloroformate

Sven Ringelband and Frank Tambornino

## Computing details

## Methyl chloroformate (srx03)

*Crystal data*

$C_2H_3ClO_2$

$M_r = 94.49$

Orthorhombic, *Pnma*

$a = 8.4404$  (5) Å

$b = 6.2019$  (4) Å

$c = 7.4314$  (4) Å

$V = 389.01$  (4) Å<sup>3</sup>

$Z = 4$

$F(000) = 192$

$D_x = 1.613$  Mg m<sup>-3</sup>

Cu *Kα* radiation,  $\lambda = 1.54186$  Å

Cell parameters from 30155 reflections

$\theta = 5.3$ – $75.7^\circ$

$\mu = 7.23$  mm<sup>-1</sup>

$T = 100$  K

Block, clear colourless

$0.30 \times 0.15 \times 0.15 \times 0.05$  (radius) mm

*Data collection*

Stoe Stadivari

diffractometer

Radiation source: microfocus sealed X-ray tube,

XENOCs GENIX 3D CU HIGH FLUX

Graded multilayer mirror monochromator

Detector resolution: 5.81 pixels mm<sup>-1</sup>

$\omega$  and  $\varphi$  scans

Absorption correction: multi-scan

(*LANA*; Koziskova *et al.*, 2016)

$T_{\min} = 0.161$ ,  $T_{\max} = 0.337$

8421 measured reflections

432 independent reflections

415 reflections with  $I > 2\sigma(I)$

$R_{\text{int}} = 0.018$

$\theta_{\max} = 75.4^\circ$ ,  $\theta_{\min} = 8.0^\circ$

$h = -8 \rightarrow 10$

$k = -7 \rightarrow 7$

$l = -9 \rightarrow 9$

*Refinement*

Refinement on  $F^2$

Least-squares matrix: full

$R[F^2 > 2\sigma(F^2)] = 0.018$

$wR(F^2) = 0.049$

$S = 1.08$

432 reflections

38 parameters

0 restraints

Primary atom site location: dual

Hydrogen site location: difference Fourier map

All H-atom parameters refined

$w = 1/[\sigma^2(F_o^2) + (0.0349P)^2 + 0.0604P]$

where  $P = (F_o^2 + 2F_c^2)/3$

$(\Delta/\sigma)_{\max} = 0.001$

$\Delta\rho_{\max} = 0.18$  e Å<sup>-3</sup>

$\Delta\rho_{\min} = -0.17$  e Å<sup>-3</sup>

*Special details*

**Geometry.** All esds (except the esd in the dihedral angle between two l.s. planes) are estimated using the full covariance matrix. The cell esds are taken into account individually in the estimation of esds in distances, angles and torsion angles; correlations between esds in cell parameters are only used when they are defined by crystal symmetry. An approximate (isotropic) treatment of cell esds is used for estimating esds involving l.s. planes.

Fractional atomic coordinates and isotropic or equivalent isotropic displacement parameters ( $\text{\AA}^2$ )

	<i>x</i>	<i>y</i>	<i>z</i>	$U_{\text{iso}}^*/U_{\text{eq}}$
Cl1	0.72372 (4)	0.750000	0.33814 (4)	0.02357 (16)
O2	0.65970 (11)	0.750000	0.66663 (10)	0.0201 (2)
O1	0.44492 (10)	0.750000	0.48536 (12)	0.0235 (2)
C1	0.58441 (15)	0.750000	0.51257 (16)	0.0179 (3)
C2	0.55644 (18)	0.750000	0.82457 (17)	0.0238 (3)
H2A	0.4907 (18)	0.622 (2)	0.8235 (14)	0.033 (3)*
H2B	0.622 (2)	0.750000	0.919 (3)	0.037 (5)*

Atomic displacement parameters ( $\text{\AA}^2$ )

	$U^{11}$	$U^{22}$	$U^{33}$	$U^{12}$	$U^{13}$	$U^{23}$
Cl1	0.0234 (2)	0.0267 (2)	0.0206 (2)	0.000	0.00467 (10)	0.000
O2	0.0148 (5)	0.0269 (5)	0.0186 (5)	0.000	0.0001 (4)	0.000
O1	0.0174 (5)	0.0283 (5)	0.0246 (5)	0.000	-0.0034 (4)	0.000
C1	0.0190 (6)	0.0154 (6)	0.0193 (6)	0.000	0.0008 (5)	0.000
C2	0.0213 (7)	0.0327 (8)	0.0174 (6)	0.000	0.0014 (5)	0.000

Geometric parameters ( $\text{\AA}$ ,  $^\circ$ )

Cl1—C1	1.7502 (13)	C2—H2A	0.968 (14)
O2—C1	1.3094 (15)	C2—H2A <sup>i</sup>	0.968 (14)
O2—C2	1.4619 (15)	C2—H2B	0.90 (2)
O1—C1	1.1945 (15)		
C1—O2—C2	114.37 (10)	O2—C2—H2A	109.6 (7)
O2—C1—Cl1	108.75 (9)	O2—C2—H2B	105.1 (12)
O1—C1—Cl1	122.47 (10)	H2A—C2—H2A <sup>i</sup>	110.1 (17)
O1—C1—O2	128.78 (11)	H2A—C2—H2B	111.2 (9)
O2—C2—H2A <sup>i</sup>	109.6 (7)	H2B—C2—H2A <sup>i</sup>	111.2 (9)
C2—O2—C1—Cl1	180.000 (1)	C2—O2—C1—O1	0.000 (1)

Symmetry code: (i)  $x, -y+3/2, z$ .

## Methyl chloroformate (srx02)

## Crystal data

 $\text{C}_2\text{H}_3\text{ClO}_2$  $M_r = 94.49$ Orthorhombic, *Pnma* $a = 8.526 (2) \text{\AA}$  $b = 6.3454 (15) \text{\AA}$  $c = 7.4619 (16) \text{\AA}$  $V = 403.67 (16) \text{\AA}^3$  $Z = 4$  $F(000) = 192$  $D_x = 1.555 \text{ Mg m}^{-3}$ Cu  $K\alpha$  radiation,  $\lambda = 1.54186 \text{\AA}$ 

Cell parameters from 21811 reflections

 $\theta = 5.9\text{--}75.5^\circ$  $\mu = 6.97 \text{ mm}^{-1}$  $T = 200 \text{ K}$ 

Block, clear colourless

 $0.30 \times 0.15 \times 0.15 \times 0.15$  (radius) mm

*Data collection*

Stoe Stadivari diffractometer	$T_{\min} = 0.231$ , $T_{\max} = 0.512$
Radiation source: microfocus sealed X-ray tube, XENOCs GENIX 3D CU HIGH FLUX	10088 measured reflections
Graded multilayer mirror monochromator	453 independent reflections
Detector resolution: 5.81 pixels mm <sup>-1</sup>	432 reflections with $I > 2\sigma(I)$
$\omega$ and $\varphi$ scans	$R_{\text{int}} = 0.022$
Absorption correction: multi-scan ( <i>LANA</i> ; Koziskova <i>et al.</i> , 2016)	$\theta_{\max} = 74.6^\circ$ , $\theta_{\min} = 7.9^\circ$
	$h = -8 \rightarrow 10$
	$k = -7 \rightarrow 7$
	$l = -9 \rightarrow 9$

*Refinement*

Refinement on $F^2$	All H-atom parameters refined
Least-squares matrix: full	$w = 1/[\sigma^2(F_o^2) + (0.0492P)^2 + 0.0148P]$
$R[F^2 > 2\sigma(F^2)] = 0.022$	where $P = (F_o^2 + 2F_c^2)/3$
$wR(F^2) = 0.064$	$(\Delta/\sigma)_{\max} < 0.001$
$S = 1.11$	$\Delta\rho_{\max} = 0.18 \text{ e } \text{\AA}^{-3}$
453 reflections	$\Delta\rho_{\min} = -0.16 \text{ e } \text{\AA}^{-3}$
39 parameters	Extinction correction: SHELXL-2018/3 (Sheldrick 2015b),
0 restraints	$\text{Fc}^* = k\text{Fc}[1 + 0.001x\text{Fc}^2\lambda^3/\sin(2\theta)]^{-1/4}$
Primary atom site location: dual	Extinction coefficient: 0.0081 (16)
Hydrogen site location: difference Fourier map	

*Special details*

**Geometry.** All esds (except the esd in the dihedral angle between two l.s. planes) are estimated using the full covariance matrix. The cell esds are taken into account individually in the estimation of esds in distances, angles and torsion angles; correlations between esds in cell parameters are only used when they are defined by crystal symmetry. An approximate (isotropic) treatment of cell esds is used for estimating esds involving l.s. planes.

*Fractional atomic coordinates and isotropic or equivalent isotropic displacement parameters ( $\text{\AA}^2$ )*

	<i>x</i>	<i>y</i>	<i>z</i>	$U_{\text{iso}}^*/U_{\text{eq}}$
C11	0.27937 (4)	0.750000	0.33697 (4)	0.0485 (2)
O2	0.34065 (11)	0.750000	0.66399 (10)	0.0382 (3)
O1	0.55347 (11)	0.750000	0.48601 (12)	0.0472 (3)
C1	0.41624 (15)	0.750000	0.51182 (15)	0.0333 (3)
C2	0.44070 (19)	0.750000	0.82207 (18)	0.0465 (4)
H2A	0.377 (3)	0.750000	0.917 (3)	0.068 (6)*
H2B	0.505 (2)	0.627 (2)	0.8228 (15)	0.064 (4)*

*Atomic displacement parameters ( $\text{\AA}^2$ )*

	$U^{11}$	$U^{22}$	$U^{33}$	$U^{12}$	$U^{13}$	$U^{23}$
C11	0.0511 (3)	0.0547 (3)	0.0396 (3)	0.000	-0.01092 (11)	0.000
O2	0.0267 (5)	0.0527 (6)	0.0352 (5)	0.000	0.0021 (3)	0.000
O1	0.0336 (5)	0.0621 (7)	0.0458 (6)	0.000	0.0086 (4)	0.000
C1	0.0334 (6)	0.0313 (6)	0.0353 (7)	0.000	0.0015 (5)	0.000
C2	0.0412 (8)	0.0649 (9)	0.0333 (7)	0.000	-0.0021 (5)	0.000

*Geometric parameters (Å, °)*

---

C11—C1	1.7504 (13)	C2—H2A	0.89 (2)
O2—C1	1.3057 (15)	C2—H2B <sup>i</sup>	0.953 (17)
O2—C2	1.4557 (16)	C2—H2B	0.953 (17)
O1—C1	1.1856 (16)		
C1—O2—C2	114.55 (11)	O2—C2—H2B	109.9 (8)
O2—C1—C11	108.61 (9)	O2—C2—H2B <sup>i</sup>	109.9 (8)
O1—C1—C11	122.46 (10)	H2A—C2—H2B	110.0 (10)
O1—C1—O2	128.93 (11)	H2A—C2—H2B <sup>i</sup>	110.0 (10)
O2—C2—H2A	106.8 (14)	H2B—C2—H2B <sup>i</sup>	110 (2)
C2—O2—C1—C11	180.000 (1)	C2—O2—C1—O1	0.000 (1)

---

Symmetry code: (i)  $x, -y+3/2, z$ .